Published in final edited form as:

J Invest Dermatol. 2022 January ; 142(1): 155–165.e3. doi:10.1016/j.jid.2021.05.029.

IFN-κ Is a Rheostat for Development of Psoriasiform Inflammation

Mehrnaz Gharaee-Kermani[1,2,8], **Shannon N. Estadt**[1,3,8], **Lam C. Tsoi**[2,4], **Sonya J. Wolf-Fortune**[1,3], **Jianhua Liu**[1], **Xianying Xing**[2], **Jonathon Theros**[1], **Tamra J. Reed**[1], **Lori Lowe**[2,5], **Dennis Gruszka**[6,7], **Nicole L. Ward**[6,7], **Johann E. Gudjonsson**[2], **J. Michelle Kahlenberg**[1,2]

[1]Division of Rheumatology, Department of Internal Medicine, Michigan Medicine, University of Michigan, Ann Arbor, Michigan, USA

[2]Department of Dermatology, Michigan Medicine, University of Michigan, Ann Arbor, Michigan, USA

[3]Graduate Program in Immunology, Michigan Medicine, University of Michigan, Ann Arbor, Michigan, USA

[4]Department of Computational Medicine and Bioinformatics, Michigan Medicine, University of Michigan, Ann Arbor, Michigan, USA

[5]Department of Pathology, Michigan Medicine, University of Michigan, Ann Arbor, Michigan, USA

[6]Department of Nutrition, School of Medicine, Case Western Reserve University, Cleveland, Ohio, USA

[7]Department of Dermatology, School of Medicine, Case Western Reserve University, Cleveland, Ohio, USA

[8]These authors contributed equally to this work.

Abstract

Correspondence: J. Michelle Kahlenberg, Division of Rheumatology, Department of Internal Medicine, Michigan Medicine, University of Michigan, 5570A MSRB 2, 1150 West Medical Center Drive, Ann Arbor, Michigan 48109-5678, USA. mkahlenb@med.umich.edu.

AUTHOR CONTRIBUTIONS

Conceptualization: MGK, SNE, SJWF, JT, JEG, JMK; Data Curation: MGK, SNE, XX, LL, LCT, JEG, JMK; Formal Analysis: MGK, SNE, LL, NLW, DG, JEG, LCT, JMK; Funding Acquisition: JMK, JEG, NLW, SNE, LCT; Investigation: MGK, XX, LL, TJR, JL; Methodology: MKG, SNE, JT, LL, SJWF, NLW, DG, JL, TJR, LCT, JEG, JMK; Project Administration: JMK; Resources: NLW, JEG, LCT, JMK; Supervision: NLW, JEG, JMK; Writing - Original Draft Preparation: MGK, SNE, JMK; Writing - Review and Editing: MGK, SNE, SJWF, JT, LCT, XX, JL, LL, TJR, DG, NLW, JEG, JMK

Data availability statement

No large-scale datasets were generated in this manuscript.

CONFLICT OF INTEREST

JEG has served on advisory boards for Almirall, Bristol Myers Squibb, Celgene, AbbVie, and Novartis. JEG has received grant support from Sun Pharma Indurstries and Almirall, and both JEG and JMK have received grant support from Celgene/ Bristol Myers Squibb and Janssen. JMK has served on advisory boards for AstraZeneca, Eli Lilly, Bristol Myers Squibb, Avion Pharmaceuticals, Provention Bio, Aurinia Pharmaceuticals, Ventus Therapeutics, and Boehringer Ingelheim. She has received grant funding from Q32 Bio. NLW has served on advisory boards for Novartis and has received grant support from Sun Pharma Industries. The remaining authors state no conflict of interest.

SUPPLEMENTARY MATERIAL

Supplementary material is linked to the online version of the paper at www.jidonline.org, and at https://doi.org/10.1016/j.jid.2021.05.029.

Psoriasis is a common, inflammatory autoimmune skin disease. Early detection of an IFN-1 signature occurs in many psoriasis lesions, but the source of IFN production remains debated. IFN-κ is an important source of IFN-1 production in the epidermis. We identified a correlation between IFN-regulated and psoriasis-associated genes in human lesional skin. We thus wanted to explore the effects of IFN-κ in psoriasis using the well-characterized imiquimod psoriasis model. Three mouse strains aged 10 weeks were used: wild-type C57Bl/6, C57Bl/6 that overexpress *Ifnk* in the epidermis (i.e., transgenic), and total body *Ifnk*$^{-/-}$ (i.e., knockout) strain. Psoriasis was induced by topical application of imiquimod on both ears for 8 consecutive days. Notably, the severity of skin lesions and inflammatory cell infiltration was more significantly increased in transgenic than in wild-type than in knockout mice. Gene expression analysis identified greater upregulation of *Mxa*, *Il1b, Tnfa, Il6*, *Il12*, *Il23, Il17,* and *Ifng* in transgenic compared to wild-type compared to knockout mice after imiquimod treatment. Furthermore, imiquimod increased CD8^{+} and CD4^{+} T-cell infiltration more in transgenic than in wild-type than in knockout mice. In summary, we identified IFN-κ as a rheostat for initiation of psoriasiform inflammation. This suggests that targeting IFN-1s early in the disease may be an effective way of controlling psoriatic inflammation.

INTRODUCTION

In total, 2−3% of the world's population is affected by psoriasis, an autoimmune skin disease characterized by epidermal hyperproliferation, abnormal differentiation of keratinocytes (KCs), and infiltration of inflammatory cells (Clark and Kupper, 2006; Li et al., 2020; Lowes et al., 2007; Nestle et al., 2009; Perera et al., 2012). The pathogenesis of psoriasis is complex, involving multiple cytokines and chemokines that promote T helper 17−mediated inflammation. Infiltration of plasmacytoid dendritic cells (DCs) and detection of an IFN-1 signature occurs early in many psoriasis lesions (van der Fits et al., 2004; Zhang, 2019), and deletion of the IFN-1 receptor is protective in imiquimod (IMQ)-induced psoriasis (Grine et al., 2015); however, the role of IFNs in and particularly the contributions of IFN-1s to psoriasis pathogenesis remain poorly understood.

Recently, we described IFN-κ as an important source of IFN-1 in the epidermis of healthy control KCs and as a contributor to inflammation and photosensitivity in systemic lupus (Sarkar et al., 2018). Reports have described both increased and decreased IFN-κ in psoriatic lesions (Li et al., 2019; Scarponi et al., 2006), but timing and location of biopsy may impact these findings. Given the potential availability of drugs that can specifically target IFN-1 signaling, it is important to understand the role of IFNs in psoriasis development to facilitate rational treatment algorithms (Lee et al., 2020; Morand et al., 2020; Shibata et al., 2015). Thus, we chose to study the responses in IMQ model of psoriasis in mice that overexpress *Ifnk* in the epidermis, under the keratin 14 promoter, and in mice that lack *Ifnk* expression and compared these with the responses noted in wild-type (WT) mice. We found that *Ifnk* expression functioned as a rheostat wherein the absence of *Ifnk* attenuated disease, and epidermal overexpression of *Ifnk* increased disease severity, recruitment of neutrophils, and production of inflammatory cytokines, including IL-17.

RESULTS

IFN-regulated genes are increased in psoriasis and correlate with *IL23* and *IL17A* expression

To better understand the role of IFNs in psoriasis, we first examined transcriptional data from 38 healthy controls and 27 nonlesional and 28 lesional biopsies from patients with psoriasis. A dramatic increase in IFN-stimulated genes was noted in the lesional psoriatic skin, whereas a subtler increase was noted in nonlesional psoriatic skin (Figure 1a). Quantification of *MX1* expression, an IFN-1−regulated gene, confirmed a significant ($P = 8 \times 10^{-3}$) but small increase in nonlesional psoriatic skin and a highly significant increase in lesional skin ($P = 1.9 \times 10^{-24}$) (Figure 1b). Although the expression of *MX1* was variable across samples, we identified correlations between the expression of psoriasis-associated cytokines (i.e., *IL23* and *IL17A*) with *MX1* only in the lesional skin (Figure 1c). Examination of transcripts for which IFN-1s were expressed in this data set identified only *IFNK* and *IFNE*. Because IFN-1s typically have low expression levels, we then examined a second data set with deeper coverage (Tsoi et al., 2015) and found *IFNK* and *IFNE* as well as *IFNA5* and *IFNA21* in a few samples. Only IFNK and IFNE showed a positive but not significant correlation with MX1 (Figure 1d). Previous literature had suggested an increase in IFN-κ as a prominent IFN in psoriatic skin, so we evaluated this by immunofluorescent staining. Indeed, MX1 was increased in psoriatic lesions, consistent with IFN-1 exposure, and an increase in IFN-κ staining was also noted (Figure 1e). These data led us to the hypothesis that *IFNK* expression may be able to modulate *IL23* and *IL17A* expression and thus act as a rheostat for psoriatic inflammation (Figure 1f).

Overexpression of IFN-κ in the epidermis enhanced IMQ-induced psoriasis

To investigate how the modulation of IFN-κ could affect the development of psoriatic inflammation, we rederived mice deficient in *Ifnk* (i.e., knockout [KO]) and generated mice that overexpress IFN-κ in the epidermis under the control of the keratin 14 promoter (i.e., transgenic [TG] mice). Absence or overexpression of *Ifnk* in murine skin was confirmed by genotyping and western blot (Supplementary Figure S1a−d). Psoriasiform inflammation was induced by treating female and male WT, *Ifnk*−TG, and *Ifnk*−KO mice aged 10 weeks with topical application of IMQ on both ears for 8 consecutive days. Untreated sex- and age-matched mice were used as controls. WT and *Ifnk*−TG mice demonstrated a significant increase in *Ifnk* expression on day 8 of treatment (Figure 2a). All IMQ-treated mice exhibited body weight loss after 2−3 days of IMQ treatment, which was improved after the addition of dietary supplements per veterinary instructions (Figure 2b). Ear lesions appeared after 4 consecutive days with IMQ treatment (representative photos of day 4 lesions are shown in Supplementary Figure S1e). Whereas all IMQ-treated mice exhibited psoriasis-like lesions in both ears after 8 days of treatment (Figure 2c), the ear thickness was significantly reduced in KO mice (blue stars) and was significantly increased in TG mice (red stars) compared with that in WT mice (Figure 2d). This suggests that baseline epidermal IFN-κ expression can regulate the inflammatory phenotype to IMQ. No differences were observed between sexes, so data from both sexes were grouped for strain-specific comparisons.

Ifnk–TG mice developed severe splenomegaly

Topical IMQ treatment is known to induce splenomegaly (Grine et al., 2016). Notably, spleen weight measured on day 9 was significantly increased in the mice after IMQ treatment in the following order: KO < WT < TG (Figure 2e and f), suggesting that the degree to which IFN-κ is present in the epidermis can also regulate the systemic response to IMQ. No sex differences were observed.

IFN-κ regulates histopathologic characteristics of psoriasis

Representative H&E-stained ear sections from KO, WT, and TG mice treated with IMQ or corresponding control are shown (Figure 3a). The scoring of epidermal scale (Figure 3b), hyperplasia (Figure 3c), dermal inflammatory infiltrate (Figure 3d), and neutrophils in scale (Munro microabscess) (Figure 3e) was completed in a blinded fashion by a dermatopathologist and revealed a subtle gradient of phenotype in IMQ-treated mice in the following order: KO < WT < TG. Acanthosis measures confirmed increases in acanthosis in IMQ-treated mice in the following order: KO < WT = TG (Figure 3f). No differences between sexes were observed. In contrast to IMQ-treated mice, untreated mice show little-to-no immune cells in ear sections.

IFN-κ overexpression enhances inflammatory cell recruitment to the skin

We then investigated whether inflammatory infiltrates were increased by the effect of IFN-κ as a result of IMQ treatment. Ear tissues were immunoassayed with anti-Ly6g, F4/80, and CD11c antibodies for detection of neutrophils, macrophages, and DCs, respectively. Increased neutrophils with larger Munro microabscesses were seen more in IMQ-treated TG mice than in WT than in KO mice. Representative images of ears stained with Ly6g are shown in Figure 4. $F4/80^+$ macrophages and $CD11c^+$ DCs were observed in greater numbers in IMQ-treated TG mice than in WT than in KO mice. In contrast, control mice showed few positive cells for all stains examined. Representative images of ear tissue stained with F4/80 and CD11c are shown in Supplementary Figure S2a and b. No differences were noted between male and female mice.

IFN-κ is a rheostat for IFN and IL-17 responses in the skin

Examination of transcriptional changes in the ears of mice on day 9 after IMQ treatment identified a more upregulation of *Mx1*, an IFN-1 response gene, in TG than in WT than in KO mice (Figure 5a). This suggests that increased IFN-κ signaling promotes IFN-1 responses, as we have previously published (Clark et al., 2015; Tsoi et al., 2019a; Wolf et al., 2019, 2018). As expected in C57Bl/6 mice (Swindell et al., 2017), IMQ also induced inflammatory genes such as *Tnfa*, *Il1b*, and *Il6* and T-cell and T helper type 17−associated response genes such as signal transducer and activator of transcription 3 gene *Stat3*, *Il23*, *Il17a*, *Il12*, and *Ifng.* In each instance, increased IFN-κ at baseline resulted in more robust upregulation, and the absence of IFN-κ dampened the upregulation of these genes after IMQ treatment (Figure 5b−i). No major differences between the sexes were noted for inflammatory gene regulation; therefore, all data were grouped for each strain. These data suggest that baseline IFN states may regulate the psoriatic inflammatory response.

IFN-κ modulates T-cell recruitment into psoriatic lesions

T cells are important pathogenic mediators in psoriasis (Di Meglio et al., 2016; Johnston et al., 2013). Given the effects of IFN-κ modulation on T-cell activators such as IFN-γ, IL-12, IL-23, and IL-1β production, we then examined the presence of $CD4^+$ and $CD8^+$ T cells in the skin of IMQ-treated mice. Ear tissue was immunostained for CD4 (Figure 6a) and CD8 (Figure 6b) and counterstained with hematoxylin (blue). More increases in $CD4^+$ and $CD8^+$ T cells were seen in IMQ-treated TG than in WT than in KO mice.

DISCUSSION

Psoriasis involves complex immunologic pathogenesis of both the innate and adaptive immune systems (Billi et al., 2019). Although our knowledge of psoriatic pathogenesis has increased in the past decade, the role of IFN-1s, specifically the role of IFN-κ, in psoriasis remains unknown (Billi et al., 2019; Crow, 2014; Eloranta and Rönnblom, 2016; Goel et al., 2020; Xin et al., 2006). In this study, we have identified that psoriasis phenotypes induced by IMQ can be lessened by the absence of IFN-κ and enhanced by increased basal IFN-κ. This suggests that modulation of the IFN state could be beneficial, especially if a patient exhibits increased IFN in the skin.

Detection of an IFN-1 signature occurs in many psoriasis lesions, and we confirmed a robust increase in IFN-regulated genes in psoriatic lesional skin. This supports the activation of this pathway in human disease; yet, the contributors to IFN-1s in human psoriasis remain unclear. In murine models, deletion of the IFN-1 receptor has been reported as protective in IMQ-induced psoriasis (Ueyama et al., 2014), but reports also suggest that the absence of IFN-1 signaling makes no difference on disease phenotype (Wohn et al., 2013). Certainly, the success of Jak inhibitors, which block IFN-1 signaling, in psoriasis is also intriguing (Punwani et al., 2012). Recently, IFN-κ has been identified to be increased in human psoriatic lesions (Li et al., 2019). Our murine-overexpressing *Ifnk*-TG mice had normal-appearing skin, suggesting that IFN-κ overexpression itself is not sufficient to induce disease. However, INF-κ had a significant potentiating effect on the production of numerous psoriasis-associated cytokines, such as IL-23 and IL-17. This was confirmed in another murine model in which subcutaneous injection of IFN-κ resulted in increased expression of *Il17* and *Tnfa* (Li et al., 2019). Thus, increased IFN-κ may set the stage for inflammatory responses. However, this role for IFN-κ does not exclude contributions from other IFN-1s, particularly IFN-ε, which was also identified to be elevated in the psoriatic human skin.

$CD11c^+$ DCs are central mediators of IMQ-induced psoriasis (Grozdev et al., 2014; Scher et al., 2019). IFN-1s have a known proinflammatory role through priming of monocytes and DCs (Ivashkiv and Donlin, 2014). IFN-1 exposure induces persistent antigen processing and class II major histocompatibility complex expression on DCs (Simmons et al., 2012). DC production of IL-23 is critical to IMQ-induced psoriasis as well. Whereas systemic administration of IFN-1s has previously been shown to downregulate DC IL-23 production and splenic T helper type 17 production (Yen et al., 2015), KCs are a robust source of IL-23 that can further trigger IL-23 production in DCs (Yoon et al., 2016). Indeed, IFN-1 stimulation causes a mild increase in *IL23* transcripts in human KCs, but in the context

of other inflammatory mediators, such as TNF-α, which is also increased by IFN-κ, KC production of IL-23 is robust (Casciano et al., 2018; Hong et al., 1999; Jiang et al., 2020; Kulig et al., 2016). Thus, our findings indicate that IFN-κ levels modulate $CD11c^+$ cell infiltrates and *IL23* transcripts suggest that IFNs function as a rheostat and may regulate the severity of psoriasis through a DC/IL-23 loop (Figure 1f). Further research is required in this regard.

In summary, IFN-1 signaling, especially the role of IFN-κ, has recently been described as an important mediator of immune responses in autoimmune diseases such as systemic lupus erythematosus. However, their role in psoriasis has not been determined. We identify a role for IFN-κ in tissue inflammation in an acute model of IMQ-induced psoriasis. After topical application of IMQ, increased epidermal overexpression of IFN-κ resulted in increased disease severity, increased production of psoriatic-associated cytokines, and more inflammatory cells recruited into the skin, including neutrophils, monocytes/macrophages, DCs, and T cells. Deletion of IFN-κ attenuated IMQ-elicited disease severity. These findings show that overproduction of IFN-1s may impact psoriasis development and that targeting IFN-1s, including IFN-κ, in early disease may reduce the inflammatory infiltrate and could potentially modulate disease flare. Further studies will need to elucidate the specific mechanisms that may be at play.

MATERIALS AND METHODS

Human skin samples and analysis

The study was approved by the University of Michigan Institutional Review Board (HUM00019384), and all patients gave written informed consent. Six-millimeter punch biopsies were taken from lesional and nonlesional skin. The study was conducted according to the Declaration of Helsinki Principles. Transcriptome data from 38 healthy controls and 28 lesional and 27 nonlesional biopsies from patients with psoriasis were obtained as previously published (Tsoi et al., 2019b). Differential expression analysis was performed comparing nonlesional with healthy control and lesional with healthy control using a negative binomial model with DESeq2 (Love et al., 2014). Comparison of cytokine expression with MX1 was undertaken using linear correlation analysis.

Mice

Female and male WT C57BL/6N mice aged 8 weeks were purchased from The Jackson Laboratory (Bar Harbor, ME). Mice deficient in *Ifnk* (*Ifnk* KO) on the C57BL/6N background were derived from The Knockout Mouse Project Repository, University of California, Davis. The genotype of these mice was confirmed by genotyping and western blotting (Supplementary Figure S1a and b). Mice TG for *Ifnk* (*Ifn*κ−TG mice) under the keratin 14 promoter (to promote epidermal overexpression) on the C57Bl/6N background were generated by Cyagen Biosciences (Santa Clara, CA) using the PiggyBac vector and confirmed by PCR. Overexpression of *Ifnk* in murine skin was confirmed by genotyping and western blotting (Supplementary Figure S1c and d). The TG and KO mice were phenotypically normal and were able to breed without difficulty. Mice were housed in the Unit for Animal Laboratory Medicine facility at the University of Michigan (Ann Arbor,

MI) under enriched conditions at a constant temperature (22−23 °C) with a 12:12-hour light-to-dark cycle and optimal humidity and free access to tap water and food ad libitum. All animal procedures were performed using protocols approved by the University of Michigan Institutional Animal Care and Use Committee on Use and Care of Animals.

IMQ-induced psoriasis

For all experiments, mice were treated at ages 9−10 weeks. The well-characterized IMQ psoriasis model was used in these studies (Lee et al., 2020; Shibata et al., 2015). Female and male WT, *Ifnk*−TG, and *Ifnk*−KO mice were randomly divided into two groups (n = 6−10 per group), and psoriasiform skin inflammation was induced using the topical application of 62 mg of Aldara cream, 5% IMQ(Valeant Pharmaceuticals North America, Bridgewater Township, NJ) per ear for 8 consecutive days. Mice were monitored daily, and ear thickness was measured with a digital caliper. Body weights and photos were taken daily. On day 9, 24 hours after the last IMQ treatment, mice were killed, and spleens were removed and weighed. Ears were removed in entirety and portioned for formalin fixation and paraffin embedding, and a small piece of tissues was mounted in Optimal Cutting Temperature Compound, and RNA isolation was performed. The treatments were completed on two separate replicate groups of mice.

Histologic analyses

A piece of the ear was fixed in 10% formalin, dehydrated, embedded in paraffin, sectioned, and stained with hematoxylin (Surgipath, 3801540, Leica Biosystems, Richmond, IL) and eosin (Surgipath, 3801600, Leica Biosystems). H&E staining was performed per standard protocols. Scoring of inflammation was conducted in a blinded fashion by a dermatopathologist (LL). Briefly, positive and negative controls were viewed for creation of scoring ranges, and then 10 images per group were assessed for alterations in epidermal scale, including the degree of hyperkeratosis and parakeratosis (scores 0−4+), with basket weave stratum corneum interpreted as normal (score = 0). Epidermal thickness was measured in millimeters with normal thickness observed in untreated specimens measuring approximately 0.02 mm and the greatest degree of epidermal hyperplasia averaging 0.12 mm. Neutrophils in the epidermis corresponding to Munro microabscesses were scored as absent or present focal or quantitated as multiple and/or excrescent collections (scores 1−4+). Scoring of dermal infiltrate was assessed similarly (scores 0−4+). Acanthosis measures were collected for the entire length of each stained section in a manner blind to mouse strain, and treatment was performed as previously described by NLW and DG (Wolfram et al., 2009).

Immunofluorescent staining

Paraffin-embedded tissue sections were heated at 60 °C for 30 minutes, deparaffinized, and rehydrated. Slides were placed in PH9 antigen retrieval buffer and heated at 125 °C for 30 seconds in a pressure cooker water bath. After cooling, slides were blocked using 10% Donkey serum (30 minutes). Overnight coincubation at 4 °C was then performed using anti-human MX1 (Abcam, Cambridge, United Kingdom; catalog number: Ab222856) at a dilution of 1:100 and anti-human IFN-κ (Abnova, Taipei City, Taiwan; catalog number: H00056832-M01) at a dilution of 1:25. Slides were then washed, incubated

with fluorescent-tag−conjugated secondary antibodies (for 30 minutes), and observed by fluorescence microscopy.

Immunohistochemistry staining

For detection of cellular populations in the skin, formalin-fixed, paraffin-embedded sections were heated at 65 °C for 30 minutes, deparaffinized, rehydrated, and heated at 100 °C for 20 minutes in pH 6 antigen retrieval buffer. Slides were washed, treated with 3% hydrogen peroxide in PBS for 5 minutes, blocked, and incubated with anti-Ly6g (1:100 dilution, ab210799, Abcam), anti-CD4 (1:50 dilutions), and anti-CD8a (1:50 dilutions, 550280, 550281, BD Pharmingen, San Diego, CA) overnight at 4 °C. Appropriate negative (no primary or secondary antibodies or isotype controls antibodies IgG, IgG2ak, and IgG2bk) were stained in parallel with each set of slides mentioned earlier. All slides were then incubated with biotinylated secondary antibodies (1:200 dilutions) (Vector Laboratories, Burlingame, CA), followed by incubation with vectastain ABC reagent and followed by detection with the diaminobenzidine reagent under a light microscope, counterstained with hematoxylin, dehydrated, and mounted. Images were acquired using a Zeiss microscope (Zeiss, Oberkochen, Germany) at indicated magnifications. Inflammatory infiltrates were quantified by taking consecutive images across the entire section of five mice per group at ×20 magnification. Positive cells were manually counted, averaged, and presented as the number of cells/×20 magnification field.

Quantitative real-time reverse transcriptase−PCR

Ear tissues were snap frozen in liquid nitrogen and stored at −80 °C until further use. Each ear was pulverized with the use of a mortar and pestle and placed in TRIzol reagent (Thermo Fisher Scientific, Waltham, MA). RNA was purified using Direct-zol RNA kits according to the manufacturer's instructions. Total RNA quantified and their purity were determined on the basis of A260 nm/A280 nm using a spectrophotometer (Thermo Fisher Scientific/NANO drop 2000). A total of 200 ng RNA was used for cDNA synthesis using a High-Capacity cDNA Reverse Transcription Kit (Applied Biosystems, Waltham, MA). Quantitative real-time reverse transcriptase−PCR was performed on a real-time PCR detection system (Bio-Rad Laboratories, Hercules, CA). Quantitative real-time reverse transcriptase−PCR was performed in technical triplicates for the biological triplicate numbers indicated in the figure legends using TaqMan Universal PCR Master Mix (Applied Biosystems). TaqMan primer sets and probes were purchased from Applied Biosystems and are listed in Supplementary Table S1. All expression values were normalized to the housekeeping gene *18S* as an internal housekeeping gene, and fold change compared with that in Vaseline-treated mice (as calculated by $2_{\wedge}$−ddCT) was plotted.

Statistics

Experimental data are presented as mean ± SEM unless otherwise indicated. All data were graphed, and statistics were performed using GraphPad Prism, version 8.0 (GraphPad Software, San Diego, CA). For data comparing multiple groups, an ordinary one-way ANOVA was used with posthoc Tukey's multiple comparisons test, unless otherwise noted. No differences were observed between male and female mice, and they were therefore grouped for strain and treatment comparisons. Comparison between the two groups was

completed by a two-tailed Student's *t*-test for normally distributed data. When there was a significant difference in variances, Welch's correction was applied. Comparisons were considered significant with a $P < 0.05$. Statistical significance levels are indicated as $*P < 0.05$, $**P < 0.01$, $***P < 0.001$, and $****P < 0.0001$.

Supplementary Material

Refer to Web version on PubMed Central for supplementary material.

ACKNOWLEDGMENTS

This work was supported by the National Institute of Arthritis and Musculoskeletal and Skin Diseases (Bethesda, MD) of the National Institutes of Health under award numbers R01-AR071384 (JMK), R01-AR060802 (JEG), P30-AR075043 (JEG and JMK), and P50-AR070590 (NLW); by the A. Alfred Taubman Medical Research Institute (Ann Arbor, MI) (JEG and JMK); by the Parfet Emerging Scholar Award (JMK); and by the National Psoriasis Foundation (JEG, NLW, LCT, and JMK).

Abbreviations:

DC	dendritic cell
IMQ	imiquimod
KC	keratinocyte
KO	knockout
TG	transgenic
WT	wild type

REFERENCES

Billi AC, Gudjonsson JE, Voorhees JJ. Psoriasis: past, present, and future. J Invest Dermatol 2019;139:e133–42. [PubMed: 31648690]

Casciano F, Pigatto PD, Secchiero P, Gambari R, Reali E. T cell hierarchy in the pathogenesis of psoriasis and associated cardiovascular comorbidities. Front Immunol 2018;9:1390. [PubMed: 29971067]

Clark KL, Reed TJ, Wolf SJ, Lowe L, Hodgin JB, Kahlenberg JM. Epidermal injury promotes nephritis flare in lupus-prone mice. J Autoimmun 2015;65: 38–48. [PubMed: 26305061]

Clark RA, Kupper TS. Misbehaving macrophages in the pathogenesis of psoriasis. J Clin Invest 2006;116:2084–7. [PubMed: 16886055]

Crow MK. Type I interferon in the pathogenesis of lupus. J Immunol 2014;192:5459–68. [PubMed: 24907379]

Di Meglio P, Villanova F, Navarini AA, Mylonas A, Tosi I, Nestle FO, et al. Targeting CD8(+) T cells prevents psoriasis development. J Allergy Clin Immunol 2016;138:274–6.e6. [PubMed: 26782974]

Eloranta ML, Rönnblom L. Cause and consequences of the activated type I interferon system in SLE. J Mol Med (Berl) 2016;94:1103–10. [PubMed: 27094810]

Goel RR, Wang X, O'Neil LJ, Nakabo S, Hasneen K, Gupta S, et al. Interferon lambda promotes immune dysregulation and tissue inflammation in TLR7-induced lupus. Proc Natl Acad Sci USA 2020;117:5409–19. [PubMed: 32094169]

Grine L, Dejager L, Libert C, Vandenbroucke RE. Dual inhibition of TNFR1 and IFNAR1 in imiquimod-induced psoriasiform skin inflammation in mice. J Immunol 2015;194:5094–102. [PubMed: 25911755]

Grine L, Steeland S, Van Ryckeghem S, Ballegeer M, Lienenklaus S, Weiss S, et al. Topical imiquimod yields systemic effects due to unintended oral uptake. Sci Rep 2016;6:20134. [PubMed: 26818707]

Grozdev I, Korman N, Tsankov N. Psoriasis as a systemic disease. Clin Dermatol 2014;32:343–50. [PubMed: 24767182]

Hong K, Chu A, Lúdvíksson BR, Berg EL, Ehrhardt RO. IL-12, independently of IFN-gamma, plays a crucial role in the pathogenesis of a murine psoriasis-like skin disorder. J Immunol 1999;162:7480–91. [PubMed: 10358203]

Ivashkiv LB, Donlin LT. Regulation of type I interferon responses. Nat Rev Immunol 2014;14:36–49. [PubMed: 24362405]

Jiang Y, Tsoi LC, Billi AC, Ward NL, Harms PW, Zeng C, et al. Cytokinocytes: the diverse contribution of keratinocytes to immune responses in skin. JCI Insight 2020;5:e142067.

Johnston A, Fritz Y, Dawes SM, Diaconu D, Al-Attar PM, Guzman AM, et al. Keratinocyte overexpression of IL-17C promotes psoriasiform skin inflammation. J Immunol 2013;190:2252–62. [PubMed: 23359500]

Kulig P, Musiol S, Freiberger SN, Schreiner B, Gyülveszi G, Russo G, et al. IL-12 protects from psoriasiform skin inflammation. Nat Commun 2016;7: 13466. [PubMed: 27892456]

Lee J, Song K, Hiebert P, Werner S, Kim TG, Kim YS. Tussilagonone ameliorates psoriatic features in keratinocytes and imiquimod-induced psoriasis-like lesions in mice via NRF2 activation. J Invest Dermatol 2020;140: 1223–32.e4. [PubMed: 31877316]

Li L, Zhang HY, Zhong XQ, Lu Y, Wei J, Li L, et al. PSORI-CM02 formula alleviates imiquimod-induced psoriasis via affecting macrophage infiltration and polarization. Life Sci 2020;243:117231. [PubMed: 31887296]

Li Y, Song Y, Zhu L, Wang X, Yang B, Lu P, et al. Interferon kappa is up-regulated in psoriasis and it up-regulates psoriasis-associated cytokines in vivo. Clin Cosmet Investig Dermatol 2019;12:865–73.

Love MI, Huber W, Anders S. Moderated estimation of fold change and dispersion for RNA-seq data with DESeq2. Genome Biol 2014;15: 550. [PubMed: 25516281]

Lowes MA, Bowcock AM, Krueger JG. Pathogenesis and therapy of psoriasis. Nature 2007;445:866–73. [PubMed: 17314973]

Morand EF, Furie R, Tanaka Y, Bruce IN, Askanase AD, Richez C, et al. Trial of anifrolumab in active systemic lupus erythematosus. N Engl J Med 2020;382:211–21. [PubMed: 31851795]

Nestle FO, Kaplan DH, Barker J. Psoriasis. N Engl J Med 2009;361:496–509. [PubMed: 19641206]

Perera GK, Di Meglio P, Nestle FO. Psoriasis. Annu Rev Pathol 2012;7:385–422. [PubMed: 22054142]

Punwani N, Scherle P, Flores R, Shi J, Liang J, Yeleswaram S, et al. Preliminary clinical activity of a topical JAK1/2 inhibitor in the treatment of psoriasis. J Am Acad Dermatol 2012;67:658–64. [PubMed: 22281165]

Sarkar MK, Hile GA, Tsoi LC, Xing X, Liu J, Liang Y, et al. Photosensitivity and type I IFN responses in cutaneous lupus are driven by epidermal-derived interferon kappa. Ann Rheum Dis 2018;77:213197.

Scarponi C, Nardelli B, Lafleur DW, Moore PA, Madonna S, De Pità O, et al. Analysis of IFN-kappa expression in pathologic skin conditions: down-regulation in psoriasis and atopic dermatitis. J Interferon Cytokine Res 2006;26:133–40. [PubMed: 16542135]

Scher JU, Ogdie A, Merola JF, Ritchlin C. Preventing psoriatic arthritis: focusing on patients with psoriasis at increased risk of transition. Nat Rev Rheumatol 2019;15:153–66. [PubMed: 30742092]

Shibata S, Tada Y, Hau CS, Mitsui A, Kamata M, Asano Y, et al. Adiponectin regulates psoriasiform skin inflammation by suppressing IL-17 production from γδ-T cells. Nat Commun 2015;6:7687. [PubMed: 26173479]

Simmons DP, Wearsch PA, Canaday DH, Meyerson HJ, Liu YC, Wang Y, et al. Type I IFN drives a distinctive dendritic cell maturation phenotype that allows continued class II MHC synthesis and antigen processing. J Immunol 2012;188:3116–26. [PubMed: 22371391]

Swindell WR, Michaels KA, Sutter AJ, Diaconu D, Fritz Y, Xing X, et al. Imiquimod has strain-dependent effects in mice and does not uniquely model human psoriasis. Genome Med 2017;9:24. [PubMed: 28279190]

Tsoi LC, Hile GA, Berthier CC, Sarkar MK, Reed TJ, Liu J, et al. Hypersensitive IFN responses in lupus keratinocytes reveal key mechanistic determinants in cutaneous lupus. J Immunol 2019a;202:2121–30. [PubMed: 30745462]

Tsoi LC, Iyer MK, Stuart PE, Swindell WR, Gudjonsson JE, Tejasvi T, et al. Analysis of long non-coding RNAs highlights tissue-specific expression patterns and epigenetic profiles in normal and psoriatic skin. Genome Biol 2015;16:24. [PubMed: 25723451]

Tsoi LC, Rodriguez E, Degenhardt F, Baurecht H, Wehkamp U, Volks N, et al. Atopic dermatitis is an IL-13−dominant disease with greater molecular heterogeneity compared to psoriasis. J Invest Dermatol 2019b;139: 1480–9. [PubMed: 30641038]

Ueyama A, Yamamoto M, Tsujii K, Furue Y, Imura C, Shichijo M, et al. Mechanism of pathogenesis of imiquimod-induced skin inflammation in the mouse: a role for interferon-alpha in dendritic cell activation by imiquimod. J Dermatol 2014;41:135–43. [PubMed: 24387343]

van der Fits L, van der Wel LI, Laman JD, Prens EP, Verschuren MC. In psoriasis lesional skin the type I interferon signaling pathway is activated, whereas interferon-alpha sensitivity is unaltered [published correction appears in J Invest Dermatol 2004;123:415]. J Invest Dermatol 2004;122:51–60. [PubMed: 14962089]

Wohn C, Ober-Blöbaum JL, Haak S, Pantelyushin S, Cheong C, Zahner SP, et al. Langerin(neg) conventional dendritic cells produce IL-23 to drive psoriatic plaque formation in mice. Proc Natl Acad Sci USA 2013;110: 10723–8. [PubMed: 23754427]

Wolf SJ, Estadt SN, Theros J, Moore T, Ellis J, Liu J, et al. Ultraviolet light induces increased T cell activation in lupus-prone mice via type I IFN-dependent inhibition of T regulatory cells. J Autoimmun 2019;103: 102291. [PubMed: 31248690]

Wolf SJ, Theros J, Reed TJ, Liu J, Grigorova IL, Martínez-Colón G, et al. TLR7-mediated lupus nephritis is independent of type I IFN signaling. J Immunol 2018;201:393–405. [PubMed: 29884703]

Wolfram JA, Diaconu D, Hatala DA, Rastegar J, Knutsen DA, Lowther A, et al. Keratinocyte but not endothelial cell-specific overexpression of Tie2 leads to the development of psoriasis. Am J Pathol 2009;174: 1443–58. [PubMed: 19342373]

Xin H, D'Souza S, Jørgensen TN, Vaughan AT, Lengyel P, Kotzin BL, et al. Increased expression of Ifi202, an IFN-activatable gene, in B6.Nba2 lupus susceptible mice inhibits p53-mediated apoptosis. J Immunol 2006;176: 5863–70. [PubMed: 16670293]

Yen JH, Kong W, Hooper KM, Emig F, Rahbari KM, Kuo PC, et al. Differential effects of IFN-β on IL-12, IL-23, and IL-10 expression in TLR-stimulated dendritic cells. J Leukoc Biol 2015;98:689–702. [PubMed: 26059829]

Yoon J, Leyva-Castillo JM, Wang G, Galand C, Oyoshi MK, Kumar L, et al. IL-23 induced in keratinocytes by endogenous TLR4 ligands polarizes dendritic cells to drive IL-22 responses to skin immunization. J Exp Med 2016;213:2147–66. [PubMed: 27551155]

Zhang LJ. Type1 interferons potential initiating factors linking skin wounds with psoriasis pathogenesis. Front Immunol 2019;10:1440. [PubMed: 31293591]

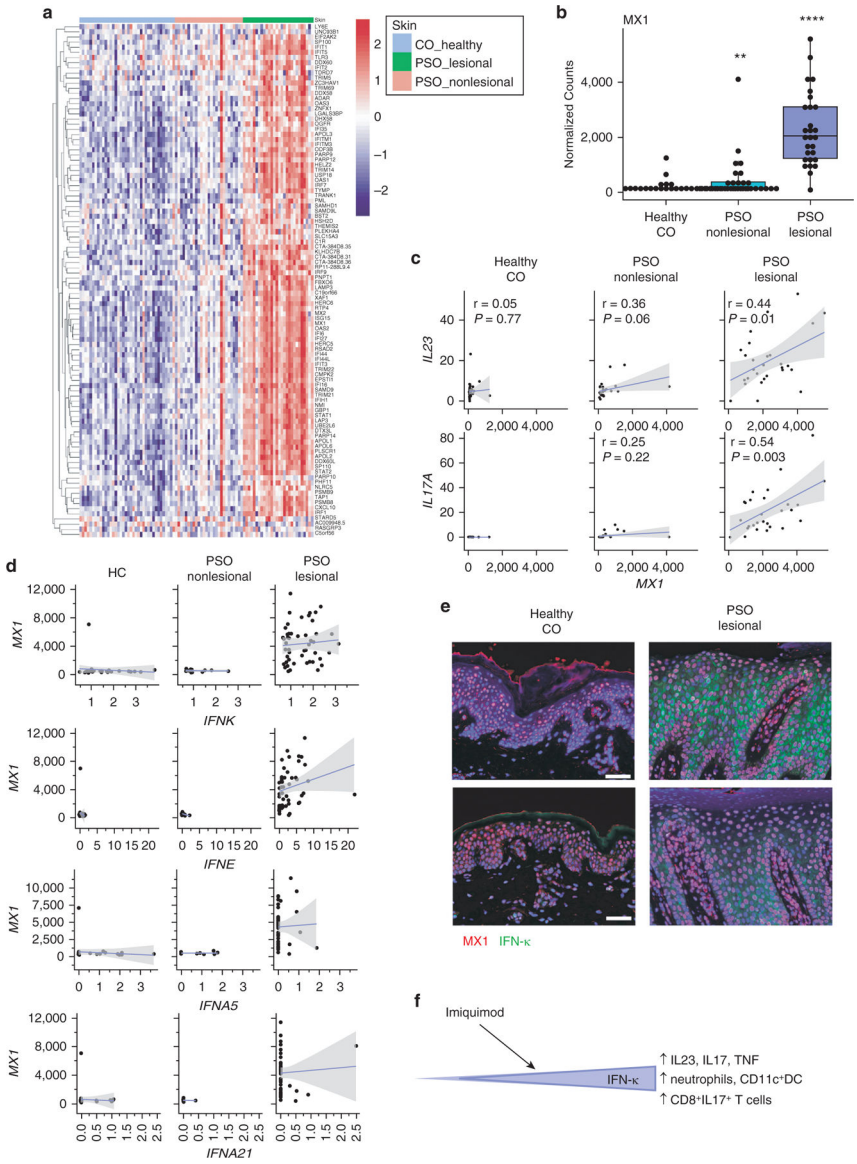

Figure 1. IFN signatures are elevated in PSO skin and correlate with *IL23* and *IL17A* expression.

(**a**) Heatmap identifying the expression of IFN-1−regulated genes in healthy CO (left, blue bar), nonlesional PSO skin (middle, pink bar), and lesional PSO skin (right, green bar). (**b**). Expression of *MX1* in the CO, nonlesional, and lesional skin. ** $P < 0.01$, **** $P < 0.0001$. (**c**). Correlations of *MX1* with *IL23* (top) and *IL17* (bottom). Pearson coefficients are shown. (**d**) Correlations of detectible *IFN1* transcripts with *MX1* in a second dataset of control and psoriasis biopsies (n = 36 healthy control, 13 nonlesional skin, and 50 lesional skin samples). (**e**) Immunofluorescent microscopy for MX1 (red) and IFN-κ (green) in two CO and lesional PSO skin biopsies. (**f**). Graded expression of IFN-κ in the epidermis regulates inflammatory mediators of psoriasis. Increasing baseline IFN-κ results in the upregulation of epidermal proliferation, cellular infiltrates, and IL-17 and IL-23 responses after imiquimod treatment. CO, control; DC, dendritic cell; PSO, psoriatic.

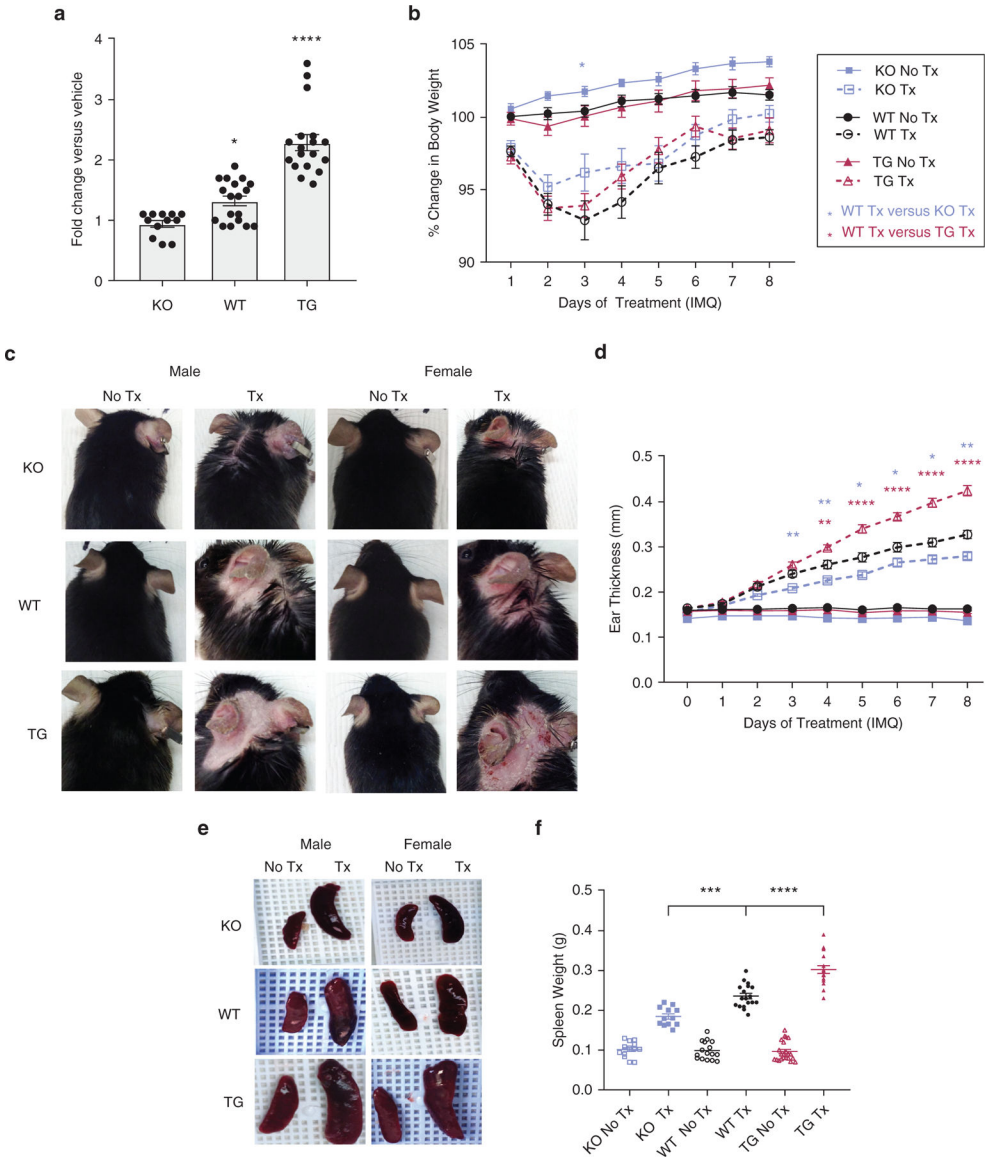

Figure 2. IFN-κ regulates IMQ-induced ear thickness and splenomegaly.

(**a**) *Ifnk* expression and (**b**) body weight after 8 days of IMQ or vehicle treatment. (**c**) Representative photographs of ears from treated and untreated male and female mice. (**d**) Change in ear thickness was assessed. n = 12−20 mice per group. * $P < 0.05$, ** $P < 0.01$, **** $P < 0.0001$. (**e**) Representative images of spleens from IMQ-treated and control mice. (**f**) Spleen weight quantitation. n = 12−20 mice per group. Statistical significance levels are indicated as *** $P < 0.001$ and **** $P < 0.0001$. IMQ, imiquimod; KO, knockout; TG, transgenic; Tx, treatment; WT, wild type.

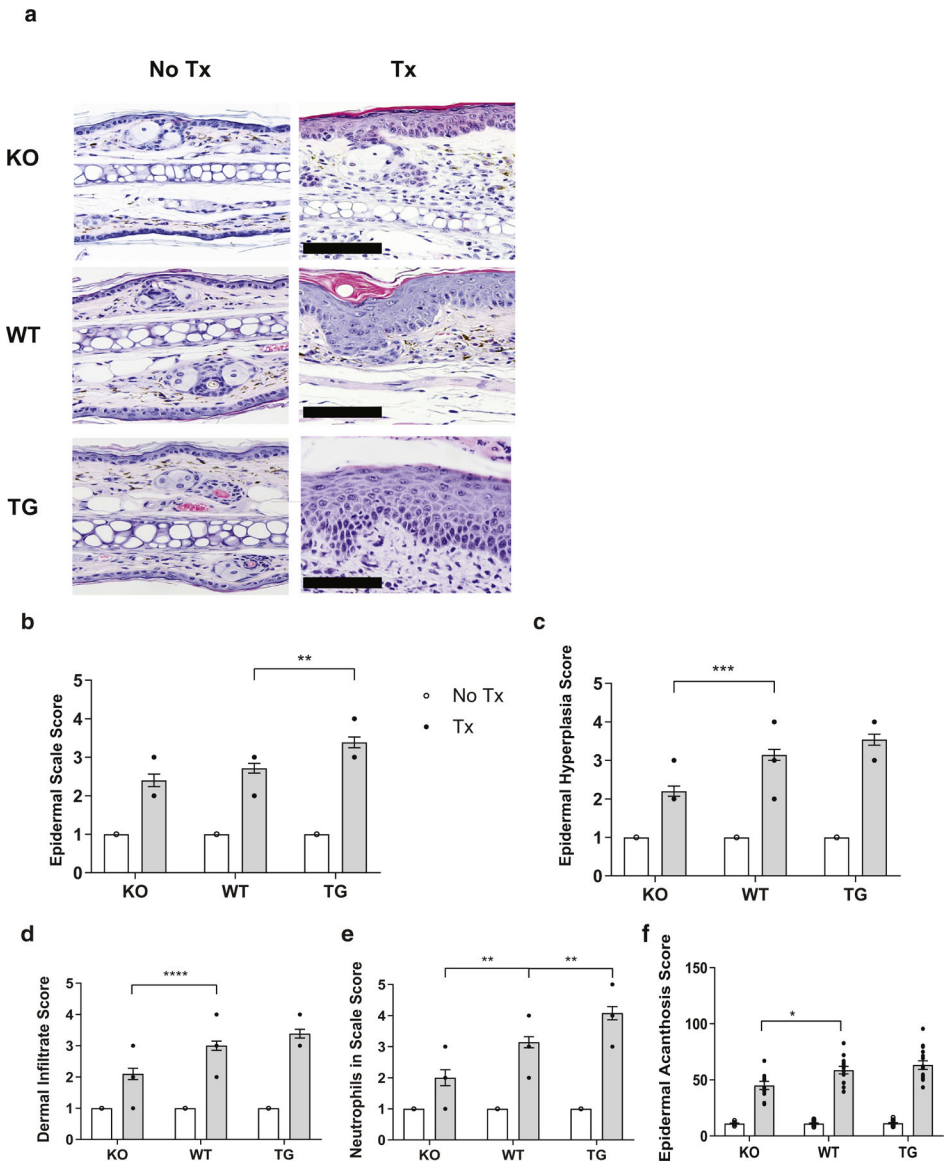

Figure 3. IFN-κ acts as a rheostat for IMQ-mediated psoriatic changes.

(**a**) Representative H&E-stained ear sections of untreated and IMQ-treated male and female mice. (**b**–**e**) Scoring of inflammation for each indicated metric was conducted in a blinded fashion by a dermatopathologist. (**f**) Average of acanthosis (in μm) across the entire ear section. Images are representative of sections from 12–20 mice per group examined. Bar = 50 μm. *$P < 0.05$; ** $P < 0.01$; ***$P < 0.001$; **** $P < 0.0001$. IMQ, imiquimod; KO, knockout; TG, transgenic; Tx, treatment; WT, wild type.

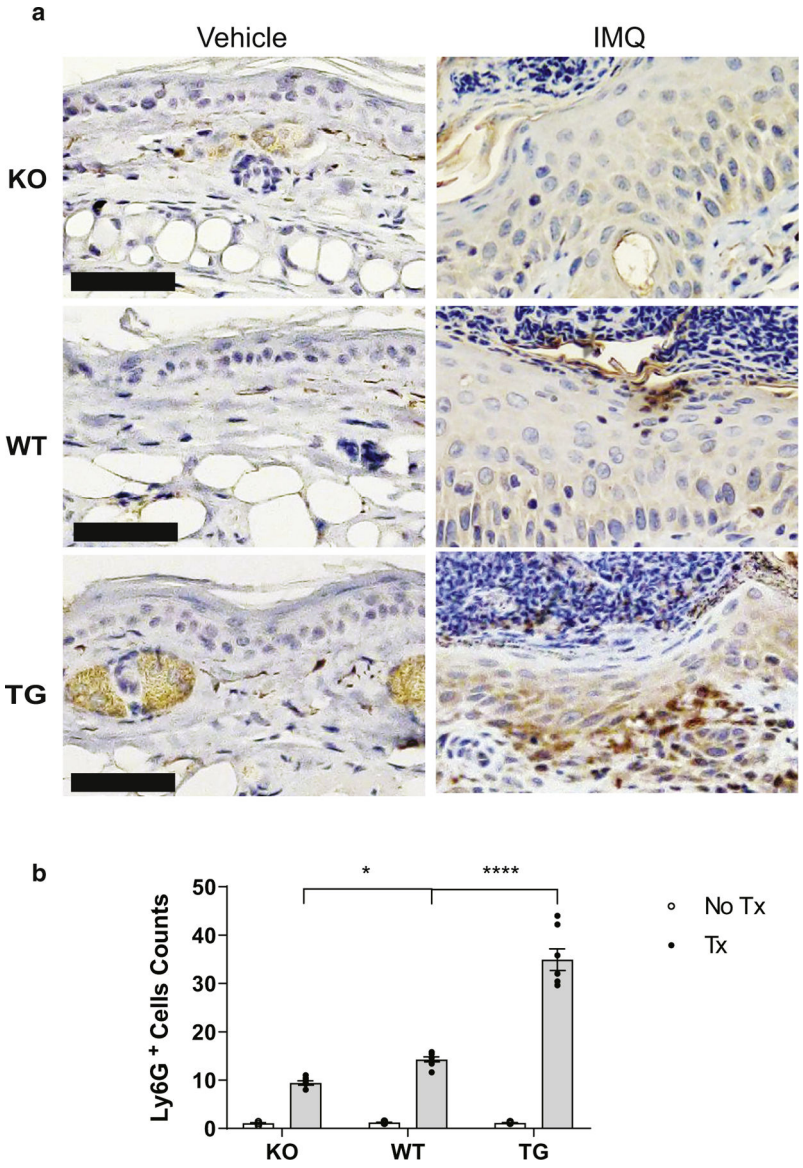

Figure 4. IFN-κ enhances neutrophil recruitment after IMQ treatment.

(**a**) Representative images of ear tissues stained with Ly6G. (**b**) Quantification of Ly6G$^+$ cells per ×20 field from images examined across the entire section from five mice in each treatment and genotype group. Bar = 50 μm. IMQ, imiquimod; KO, knockout; TG, transgenic; Tx, treatment; WT, wild type.

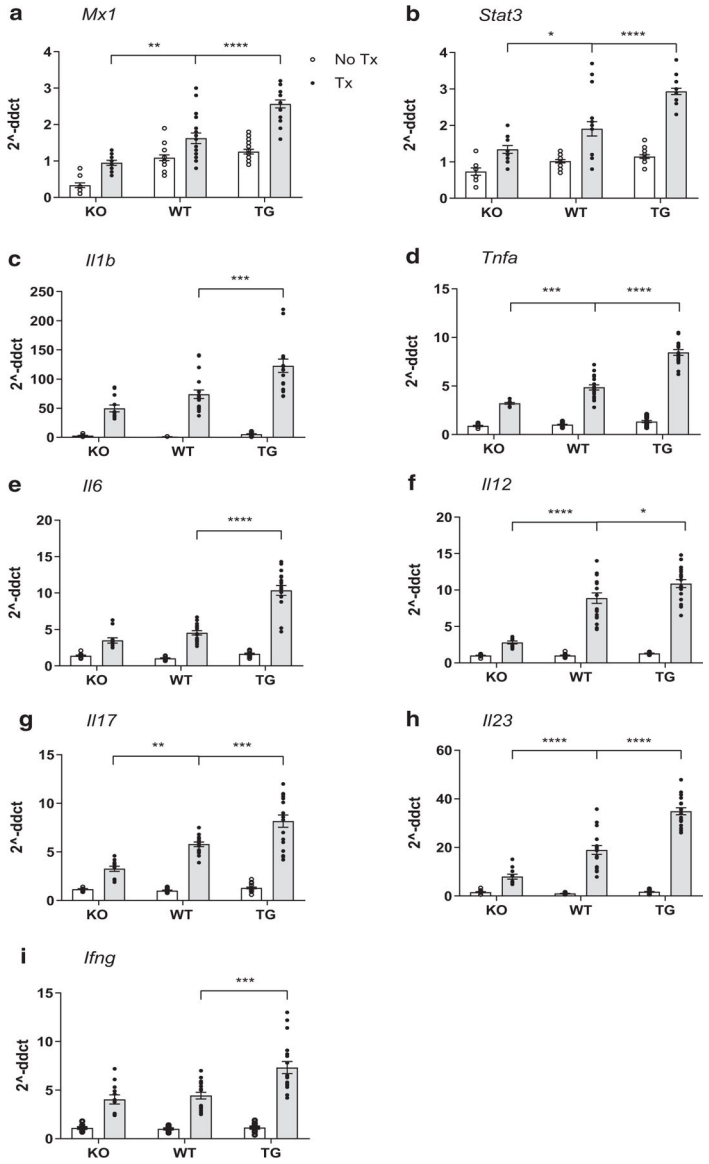

Figure 5. IFN-κ enhances IFN-1 and psoriasis-associated cytokine transcripts.

IFN-1−regulated genes (**a**) *Mx1* and (**b**) STAT3 mRNA *Stat3* expression; (c−e) inflammatory genes, including *Tnfa, Il1b,* and *IL6*; and (f−i) Th17-associated response genes, including *Il23, Il17a, Il12,* and *Ifng* mRNA expression are shown from IMQ-treated and -untreated mice. QRT-PCR was performed in technical triplicates. Data are represented as mean ± SEM. Statistics were calculated by one-way ANOVA with Tukey's correction for multiple comparisons or nonparametric Mann−Whitney U test. *$P < 0.05$; ** $P < 0.01$; *** $P < 0.001$; **** $P < 0.0001$. Each dot represents the average technical triplicate for a single mouse (n = 12−20 per group). IMQ, imiquimod; KO, knockout; QRT-PCR, quantitative real-time reverse transcriptase−PCR; STAT3, signal transducer and activator of transcription 3; TG, transgenic; Th17, T helper type 17; Tx, treatment; WT, wild type.

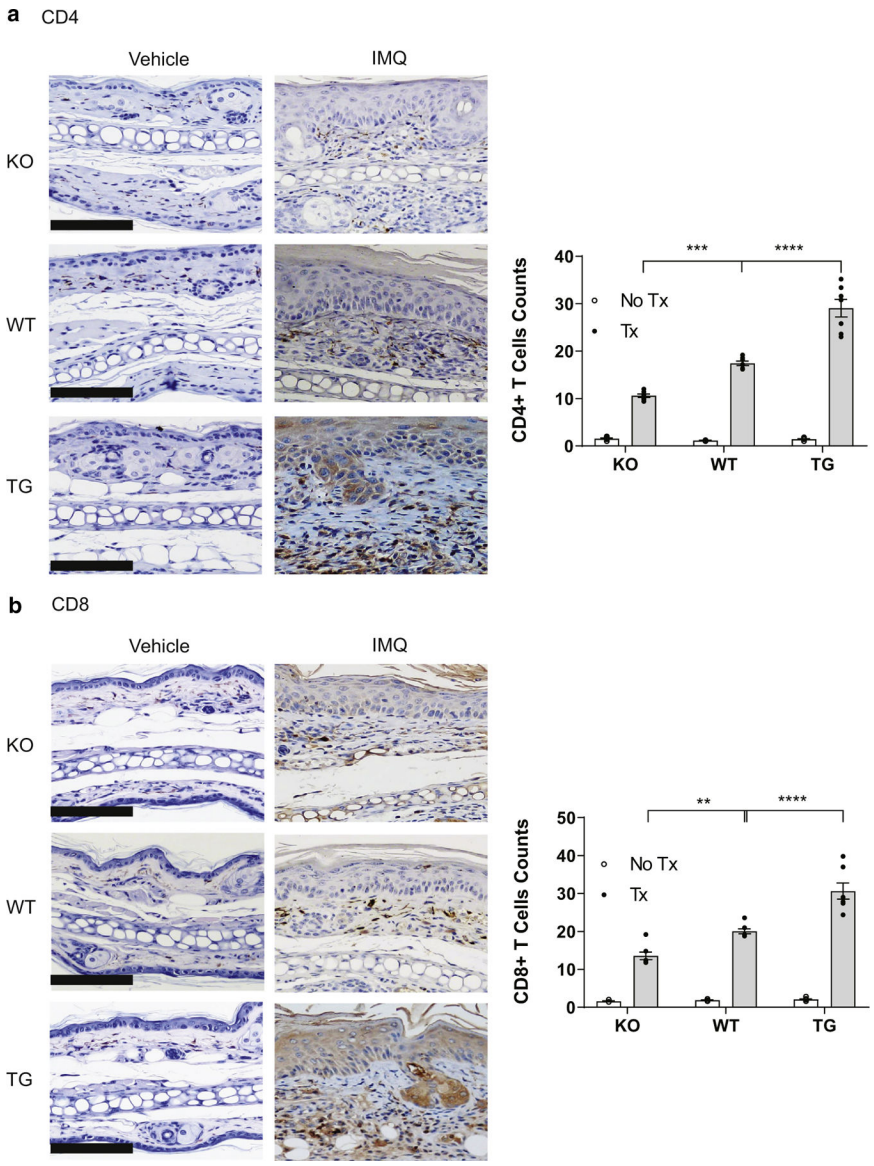

Figure 6. IFN-κ drives T-cell recruitment to psoriatic lesions.

(**a**) Representative images of KO, WT, and TG mice treated with IMQ stained for (**a**) CD4 and (**b**) CD8. Left panels show representative images; right panel shows the quantification of (**a**) CD4- and (**b**) CD8-positive cells per ×20 field from images examined across the entire section from five mice in each treatment and genotype group. Bar = 50 μm. Bar = 50 μm. IMQ, imiquimod; KO, knockout; TG, transgenic; Tx, treatment; WT, wild type.